Journal of Dental Research
2022, Vol. 101(8) 931–941

DOI: 10.1177/00220345221075215
journals.sagepub.com/home/jdr

Gnas Loss Causes Chondrocyte Fate Conversion in Cranial Suture Formation

R. Xu[1,2], Y. Liu[1], Y. Zhou[1], W. Lin[2], Q. Yuan[2], X. Zhou[2], and Y. Yang[1]

Abstract

Calvaria development is distinct from limb formation. Craniosynostosis is a skull deformity characterized by premature cranial suture fusion due to the loss of the *GNAS* gene and, consequently, its encoded protein $G\alpha_s$. This birth defect requires surgery, with potential lethal consequences. So far, hardly any early-stage nonsurgical interventions for *GNAS* loss-related craniosynostosis are available. Here, we investigated the role of the *Gnas* gene in mice in guarding the distinctiveness of intramembranous ossification and how loss of *Gnas* triggered endochondral-like ossification within the cranial sutures. Single-cell RNA sequencing (scRNA-seq) of normal neonatal mice cranial suture chondrocytes showed a Hedgehog (Hh) inactivation pattern, which was associated with $G\alpha_s$ signaling activation. Loss of *Gnas* evoked chondrocyte-to-osteoblast fate conversion and resulted in cartilage heterotopic ossification (HO) within cranial sutures and fontanels of the mouse model, leading to a skull deformity resembling craniosynostosis in patients with loss of *GNAS*. Activation of ectopic Hh signaling within cranial chondrocytes stimulated the conversion of cell identity through a hypertrophy-like stage, which shared features of endochondral ossification in vivo. Reduction of *Gli* transcription activity by crossing with a loss-of-function *Gli2* allele or injecting GLI1/2 antagonist hindered the progression of cartilage HO in neonatal stage mice. Our study uncovered the role of $G\alpha_s$ in maintaining cranial chondrocyte identity during neonatal calvaria development in mice and how reduction of Hh signaling could be a nonsurgical intervention to reduce skull deformity in craniosynostosis due to loss of *GNAS*.

Keywords: craniofacial anomalies, craniofacial biology/genetics, developmental biology, cell differentiation, signal transduction, translational medicine

Introduction

Calvaria bone formation is distinct from long bone development. During development, calvaria bone elements go through intramembranous ossification to form cranial sutures rather than endochondral ossification (Minoux et al. 2017). The essential difference lies in whether the ossification results from the cartilage template or not (Newton et al. 2019). It is generally accepted that craniofacial bones develop from the cranial neural crest and head mesoderm, while limb buds originate from an ectoderm cover with a mesoderm core (Martik et al. 2019). The question of whether the distinctiveness of calvaria bone formation is maintained by a specific gene during development has remained unanswered.

Normally, the skull vault develops from scattered ossification centers and expands as bone elements, which meet as patent sutures or fontanels (Warren et al. 2003). Human cranial sutures fuse after 20 y of age, while mice cranial sutures remain patent throughout the majority of their life (Massimi et al. 2019). Pathologically, premature fusion of cranial sutures or fontanels results in craniosynostosis, commonly caused by congenital disorders, of which the clear mechanisms are still unknown. Innovative mesenchymal stem cell–based suture regeneration in adult mice has inspired this field of research (Yu et al. 2021), where nonsurgical approaches in neonatal mice are yet to be explored.

Collectively, genetic-based rare diseases are not infrequent (Fresard et al. 2019), but nonsurgical approaches or definitive therapeutic interventions remain a challenge with our current knowledge (Tambuyzer et al. 2020). $G\alpha_s$, encoded by the *GNAS* gene in humans, is the stimulatory alpha subunit of the heterotrimeric G protein that transduces signals from G protein–coupled receptors (GPCRs) (Hu and Shokat 2018).

[1]Department of Developmental Biology, Harvard School of Dental Medicine, Harvard Stem Cell Institute, Boston, MA, USA
[2]State Key Laboratory of Oral Diseases, National Clinical Research Center for Oral Diseases, West China Hospital of Stomatology, Sichuan University, Chengdu, China

A supplemental appendix to this article is available online.

Corresponding Authors:
X. Zhou, State Key Laboratory of Oral Diseases, National Clinical Research Center for Oral Diseases, West China Hospital of Stomatology, Sichuan University, No. 14, 3rd Section of Ren Min Nan Rd, Chengdu, Sichuan 610041, China.
Email: Zhouxd@scu.edu.cn
R. Xu, State Key Laboratory of Oral Diseases, National Clinical Research Center for Oral Diseases, West China Hospital of Stomatology, Sichuan University, No. 14, 3rd Section of Ren Min Nan Rd, Chengdu, Sichuan 610041, China.
Email: Xurs@scu.edu.cn

Gain-of-function mutations in the *GNAS* gene cause fibrous dysplasia/McCune-Albright syndrome (OMIM #174800), a rare, prevalently malignant disease (Hagelstein-Rotman et al. 2021). Loss-of-function mutations in the *GNAS* gene cause progressive osseous heteroplasia (POH) (OMIM #166350), Albright hereditary osteodystrophy (AHO, OMIM #103580), or pseudo-pseudohypoparathyroidism (PPHP, OMIM #612 463) (Shore et al. 2002), three rare autosomal dominant disorders. Loss of *GNAS* is characterized by progressive heterotopic ossification (HO) in extraskeletal soft tissue (Cong et al. 2021). Although only a few clinical craniosynostosis cases due to loss of *GNAS* have been reported, infantile lethal cerebral infarction after surgery was documented (Leclercq et al. 2018). In mice, it is assumed that skull deformity due to the loss of *Gnas* results from altered or accelerated mesenchymal progenitor/stem cell specification or commitment (Xu, Khan, et al. 2018). Conversely, expression of *Gnas* with a gain-of-function mutation caused abnormal cartilage development in mouse limbs, resembling enchondroma-like lesions (Khan et al. 2018). Key decisions on cell fate occur early in embryonic development (Frost et al. 2021). We have previously reported that loss of *Gnas* leads to Hedgehog (Hh) activation (Xu, Khan, et al. 2018), which not only is crucial for skeletal development but has also been found essential in cell fate decisions (Vercauteren Drubbel et al. 2021). Mechanisms of fate decision and possible nonsurgical methods to alleviate skull deformity in craniosynostosis due to loss of *Gnas* in the early developmental period of mice have yet to be determined.

In this study, we used a mouse model to elucidate the role of $G\alpha_s$ in the distinction of cranial chondrocytes during intramembranous ossification in calvaria development. When *Gnas* was lost, mutant cranial chondrocytes went autonomously through hypertrophy and ossified to strengthen HO within cranial sutures and fontanels. Activation of Hh signaling in cranial chondrocytes, mostly in a ligand-independent manner, stimulated this identity conversion. Reduction of Hh signaling, either genetically or by using inhibitors, decreases cranial chondrocyte conversion and cartilage HO. Our findings indicate cell fate conversion during the neonatal period as a distinctive complement to the mechanism of craniosynostosis due to loss of *Gnas*. Correcting Hh signaling might be a promising nonsurgical approach to prevent skull deformity in craniosynostosis from expanding progressively at an early stage in POH, AHO, and PPHP patients due to loss of *GNAS*.

Materials and Methods

Mice

The study conforms to the ARRIVE (Animal Research: Reporting of In Vivo Experiments) guidelines. Animal care and experiments were performed in accordance with the Institutional Animal Care and Use Committee (IACUC) guidelines at the National Institutes of Health and the Harvard Medical School, protocol number 05163 (Yingzi Yang). All mice were housed in specific pathogen-free conditions and kept in the Harvard animal facilities. Pregnant mice were housed separately in a temperature-controlled (25°C) environment under a 12-h light/dark cycle, with cotton batting, and fed a rodent chow diet (5058; Pico Lab). Both male and female pups were included in our studies, showing no difference in suture formation. All pups within minimum sample size were euthanized and harvested with care for analysis at the neonatal stage. All pups were taken special care of and specifically monitored twice a day. All mice are described in published literature: *Prrx1-Cre* (Logan et al. 2002), $Gnas^{fl/fl}$ (Chen et al. 2005), *Sox9-CreER* (Soeda et al. 2010; Ono et al. 2014), $Ptch1^{LacZ/+}$ (Mak et al. 2006), $Gli2^{fl/fl}$ (Corrales et al. 2006), and *Osx-Cre* (Rodda and McMahon 2006). $R26R^{tdTom}$ (JAX007914) mice were purchased from Jackson Laboratory.

Histology

Mouse calvarias were carefully dissected and fixed in freshly made 4% paraformaldehyde, overnight at 4°C, then decalcified in 20% EDTA for 1 to 5 d. Specimens were processed in 30% sucrose at 4°C. Specimens were carefully positioned and embedded in optimal cutting temperature (OCT) compound under a stereoscope and sectioned at a 6-mm thickness (Leica CM3050S). Slides were stained with 1% silver nitrate solution under a 60-W lamp for 1 h, then rinsed in distilled water and washed with 5% sodium thiosulfate. Slides were soaked in distilled water and counterstained with 1% Safranin O or fast red, then rinsed in 1% acetic acid or distilled water before mounting. Images were captured with a light microscope (Olympus, BX51) and the cellSens software (Olympus).

Results

The Distinctiveness of Cranial Cartilage Is Associated with $G\alpha_s$ Signaling

To unveil the unique activation pattern of Hh signaling in intramembranous and endochondral ossification during bone development, we retrieved online single-cell RNA sequencing (scRNA-seq) data sets (Holmes et al. 2020; Kelly et al. 2020) of cranial sutures and limbs at E18.5 for comparative analysis. The cranial suture and limb cell populations were divided into mesenchymal population, chondrocytes, osteoblasts, and other cells indicated by a UMAP plot. The number of $Gli1^+$ and *Patched-1*$^+$ ($Ptch1^+$) (Gong et al. 2018) cranial osteoblasts was higher than chondrocytes, indicating that Hh signaling was distinctively activated in the osteoblasts of intramembranous ossification during calvaria development (Fig. 1A). Conversely, the amount of $Gli1^+$ and $Ptch1^+$ limb chondrocytes was higher than limb osteoblasts, suggesting that chondrocyte Hh signaling activation was dominant during limb development (Fig. 1B). We confirmed this converse Hh signaling pattern by using mice with the $Ptch1^{LacZ}$ allele—an in vivo readout of Hh activation (Xu, Khan, et al. 2018), as *Ptch1* is a transcriptional target of Hh signaling. X-gal staining was positive in cranial osteoblasts but negative in cranial suture chondrocytes, as well

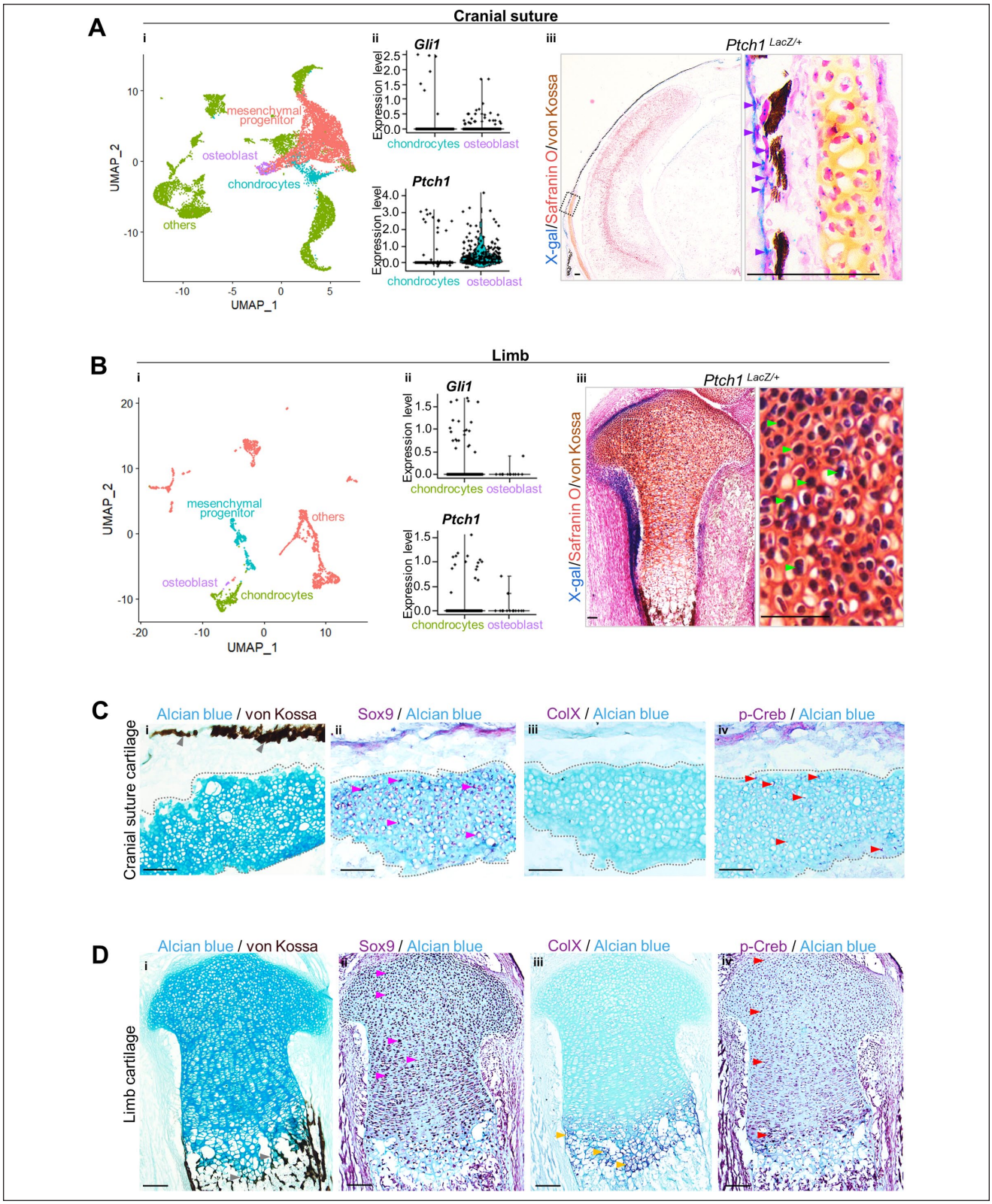

Figure 1. The distinctiveness of cranial cartilage is associated with $G\alpha_s$ signaling. (**A**, **B**) i: Cell populations of cranial sutures and limbs at E18.5 identified by online single-cell RNA sequencing data sets are visualized with UMAP. Clusters of mesenchymal progenitors, chondrocytes, osteoblasts, and others are defined in a descending order by color (pink, green, blue to purple). ii: Violin plot for the expression levels of *Gli1* and *Ptch1*. iii: X-gal$^+$ osteoblasts (purple arrow) or chondrocytes (green arrow) are indicated in a stained section from *Ptch1*^{LacZ} mice. Scale bar: 100 μm. (**C**, **D**) Immunostaining using Sox9, collagen type X (ColX), and phosphorylated-Creb (p-Creb) antibodies on a sagittal section of mastoid fontanel and femur, respectively, from mice at P0. (i–iv) Immunohistochemistry staining with the indicated antibodies counterstained with Alcian blue on cranial suture cartilage or limb. ColX$^+$ hypertrophic limb chondrocytes (yellow arrow), p-Creb$^+$ cranial suture cartilage, and limb chondrocytes except in the hypertrophic zone (red arrow); mineralization (gray arrow) is indicated in Sox9$^+$ chondrocytes (pink arrow). Scale bar: 50 μm.

as high in limb chondrocytes compared with limb osteoblasts (Fig. 1A, B). This indicated that cranial and limb chondrocytes were distinct.

Next, we found that such distinctive activation of Hh signaling is associated with $G\alpha_s$ signaling in mice at postnatal day 0 (P0). Cranial cartilage (Alcian blue staining) was beneath the bone elements (von Kossa staining) during intramembranous ossification, while limb cartilage contributed to mineralization through hypertrophy (Fig. 1C, D). Sox9 is a marker for total chondrocytes, collagen type X (ColX) is for chondrocyte hypertrophy, and phosphorylated-Creb (p-Creb) is the readout of $G\alpha_s$ signaling activation. Cranial cartilage showed uniformity of p-Creb$^+$/Sox9$^+$ double-positive suture chondrocytes, all of which did not express ColX or ossification (Fig. 1C). Limb cartilage showed a classic expression pattern of Sox9 and ColX in a chronological and spatially sequential manner, where the expression pattern of p-Creb was relatively mutually independent of ColX, which contributed to endochondral ossification (Fig. 1D). It is suggested that $G\alpha_s$ signaling might be key in cranial chondrocytes to avoiding endochondral-like conversion during intramembranous ossification.

Loss of Gnas *in Osteochondral Progenitor Cells Caused Cartilage Mineralization in the HO of Cranial Sutures and Fontanels*

We crossed mice with floxed loss-of-function *Gnas* alleles (Chen et al. 2005) with the *Prrx1-Cre* line (Logan et al. 2002) to delete *Gnas* from cranial osteochondral progenitor cells in the skull vault region; the aim was to characterize defects of cranial bone and suture formation, caused by loss of *Gnas* in the developmental stages. Due to severe cranial and limb skeletal phenotype, most of the mutant mice died after P6, and P6 and P14 pups especially received diligent care and were harvested with particular care. Using micro–computed tomography (micro-CT) scanning and 3-dimensional reconstruction of mouse calvarias at P14, we found that *Prrx1-Cre; Gnas$^{fl/fl}$* mice showed heterotopic ossification within the sagittal suture, posterior fontanel, lambdoid suture, and mastoid fontanel ($n = 6$, 100% of mutant mice showed suture HO), compared with the calvarias from control littermates of the *Prrx1-Cre; Gnas$^{fl/+}$*, *Gnas$^{fl/fl}$*, or *Gnas$^{fl/+}$* mice, which were phenotypically indistinguishable from wild-type specimens (Fig. 2A). The mutant calvarias exhibited premature closure of cranial sutures, which resembled the craniosynostosis reported in patients with *GNAS* loss-of-function mutations (Graul-Neumann et al. 2009).

We then focused on the neonatal stage of *Prrx1-Cre; Gnas$^{fl/fl}$* mice in a subsequent analysis and performed histological analyses of the ectopic ossification within sutures; however, the earliest phenotype was observed in the E16.5 section but not in whole-mount skeletal staining (Appendix Fig. 2A). Whole-mount skeletal staining of the skeletal preparation allowed the visualization of cartilage and mineralized tissues, respectively. At P0, cranial cartilage mineralization in the calvaria of mutants occupied approximately 50% of the indicated cartilage area (Fig. 2B, C, Appendix Fig. 3). By double staining with Safranin O and von Kossa, mutant chondrocytes were found to be hypertrophic-like and mineralized (Fig. 2D, blue arrows) compared with normal chondrocytes in the controls. These data indicate that loss of *Gnas* altered the status of cranial cartilage during calvaria bone formation at the neonatal stage.

To further investigate the potential transdifferentiation of chondrocytes into osteoblasts, we crossed *R26R^{tdTom}* reporter mice with *Prrx1-Cre; Gnas$^{fl/fl}$* mice, labeling mutant cells as tdTomato$^+$ (tdTom$^+$) (Fig. 2E). Osteopontin (OPN) is expressed by mature hypertrophic chondrocytes and osteoblasts. Immunostaining revealed that normal tdTom$^+$ cells in the evaluated cranial cartilage did not express ColX, Osterix (Osx), or OPN (Fig. 2E, Appendix Fig. 4A–F). However, tdTom$^+$ mutant chondrocytes presented an increased expression of ColX, Osx, and OPN (Fig. 2E, Appendix Fig. 4A–F). No tdTom$^-$ chondrocytes expressed osteogenic markers, suggesting that loss of *Gnas* within chondrocytes resulted in their transdifferentiation into an osteogenic lineage through hypertrophy.

Sox9$^+$ Chondrocyte-Specific Loss of Gnas *Recapitulated Cranial Cartilage HO and Chondrocyte-Osteoblast Conversion*

As *Prrx1-Cre* is active in mesenchymal progenitor cells, we generated Sox9$^+$ chondrocyte-specific loss of *Gnas* by crossing the *Sox9-CreER* line with *R26R^{tdTom}* reporter and *Gnas$^{fl/fl}$* alleles to evaluate the specific function of *Gnas* in chondrocytes (Fig. 3A, B, Appendix Fig. 4G). The earliest phenotype was observed in E16.5 (Appendix Fig. 2A) when tamoxifen was injected. The disappearance or removal of the cranial cartilage started from the anterior apical region toward the basal posterior portions, the last of which disappeared around P10 (Holmbeck et al. 2003). To elucidate chondrocyte fate (Appendix Fig. 2B), P6 was chosen to illustrate fate transformation in *Sox9-CreER; Gnas$^{fl/fl}$* mice. After induction, P6 calvaria with loss-of-function *Gnas* mutation revealed that the mice had recapitulated ectopic mineralization within the cartilage of the mastoid fontanel (Fig. 3C, indicated by yellow arrow). Through immunostaining, we found that neither Osx nor OPN was expressed by chondrocytes that had been effectively labeled by tdTom in the normal control mastoid cartilage of *Sox9-CreER; R26R^{tdTom}* mice (Fig. 3C). The mutant mastoid cartilage of *Sox9-CreER; R26R^{tdTom}*; *Gnas$^{fl/fl}$* mice showed ectopic Osx expression in ~40% of tdTom$^+$ chondrocytes and OPN expression in ~30% of tdTom$^+$ chondrocytes (Fig. 3D). Three-dimensional reconstruction of micro-CT–scanned P14 calvarias showed the presence of ectopic bone in the sagittal suture, posterior fontanel, and mastoid fontanel, while the control suture remained patent (Fig. 3E). Thereafter, we crossed *Osx-Cre* mice with *Gnas$^{fl/fl}$* mice to investigate the impact of mutant osteoblasts on chondrocyte fate. No cartilage mineralization or premature fusion of sutures and fontanels was identified in the calvarias of *Osx-Cre; Gnas$^{fl/fl}$* mice at P0, compared with calvarias of the control *Osx-Cre* mice (Wang et al. 2015) (Appendix Fig. 1A). Therefore, we suggest that suture fusion is the result of HO of suture mesenchymal progenitor cells and cartilage.

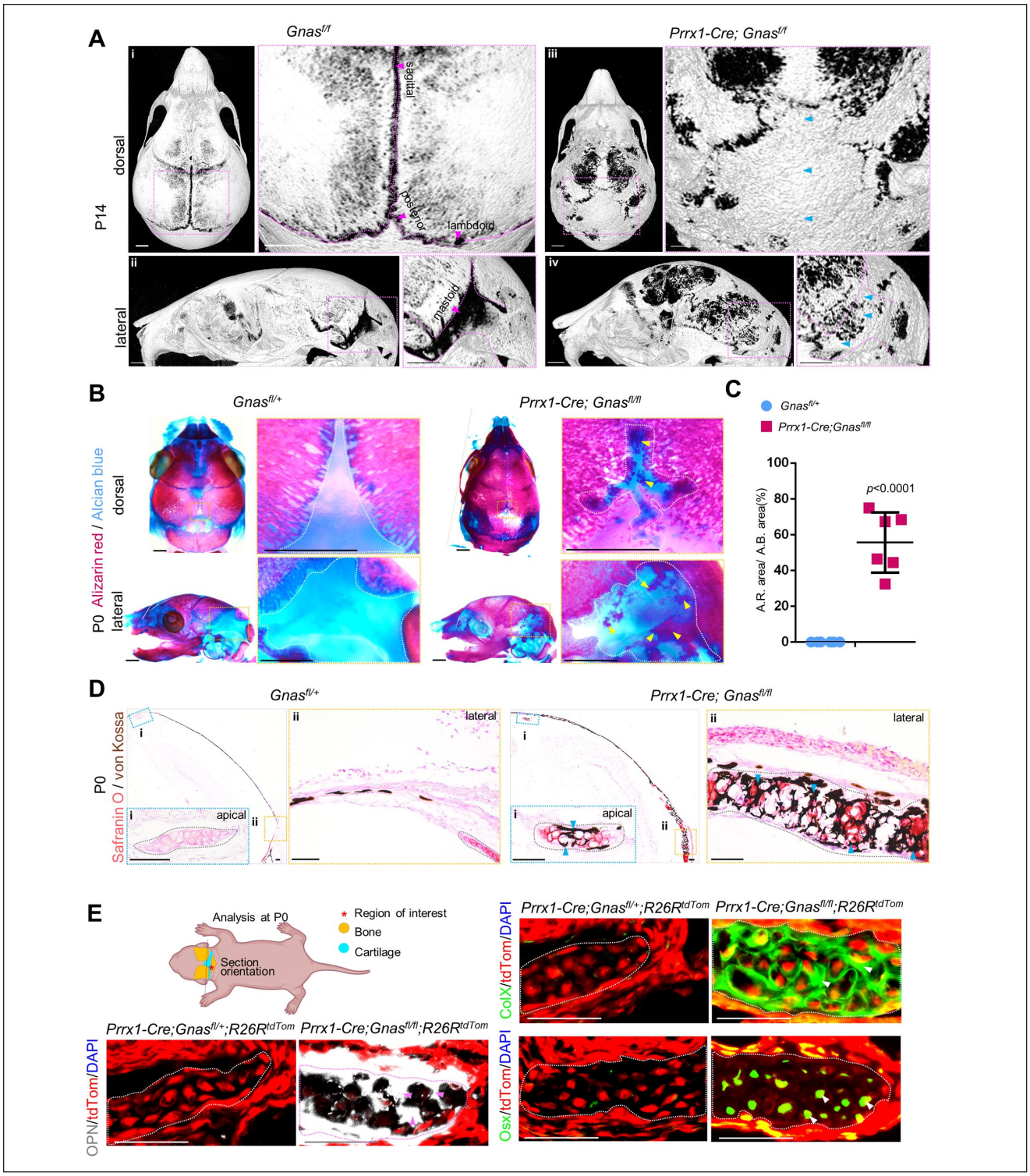

Figure 2. Loss of *Gnas* in osteochondral progenitor cells caused cartilage mineralization in the heterotopic ossification (HO) of cranial sutures and fontanels. (**A**) Micro–computed tomography 3-dimensional reconstruction image of control calvarias and *Prrx1-Cre; Gnas*$^{fl/fl}$ calvarias at P14. *N* = 6. Blue arrows indicate HO. Scale bar: 1 mm. (**B**) Skeletal preparation of calvarias of controls and *Prrx1-Cre; Gnas*$^{fl/fl}$ at P0. Dotted lines (white) outline the cranial cartilage. The arrow (yellow) indicates mineralization within the cartilage. (**C**) Quantification based on skeletal preparation. Percentage of the Alizarin red area among total Alcian blue area of mastoid fontanels at P0. *N* = 6 mastoid fontanels from 6 mice. A.R. area/A.B. area: percentage of area of Alizarin red–positive tissue within cartilage out of area of Alcian blue–positive tissue. Mean ± SD. Two-tailed *t* test. (**D**) Costaining with Safranin O (orange to red) and von Kossa (brown to black) on coronal sections from control and *Prrx1-Cre; Gnas*$^{fl/fl}$ mutant mice at P0. Dotted lines (gray) outline cranial cartilage. The arrow (blue) indicates ectopic mineralization within the cartilage. Scale bar: 100 μm. (**E**) Schematics of analysis, as well as immunofluorescence staining of *Prrx1-Cre; Gnas*$^{fl/fl}$; *R26R*^{Tomato} and controls using antibodies for collagen type X (ColX), Osterix (Osx), and osteopontin (OPN) at P0. Tomato labels mutant cells (red). Osteogenic differentiated status (arrows indicate ColX [green], Osx [green], OPN [white]) is indicated in the outlined mutant cranial cartilage. Scale bar: 50 μm.

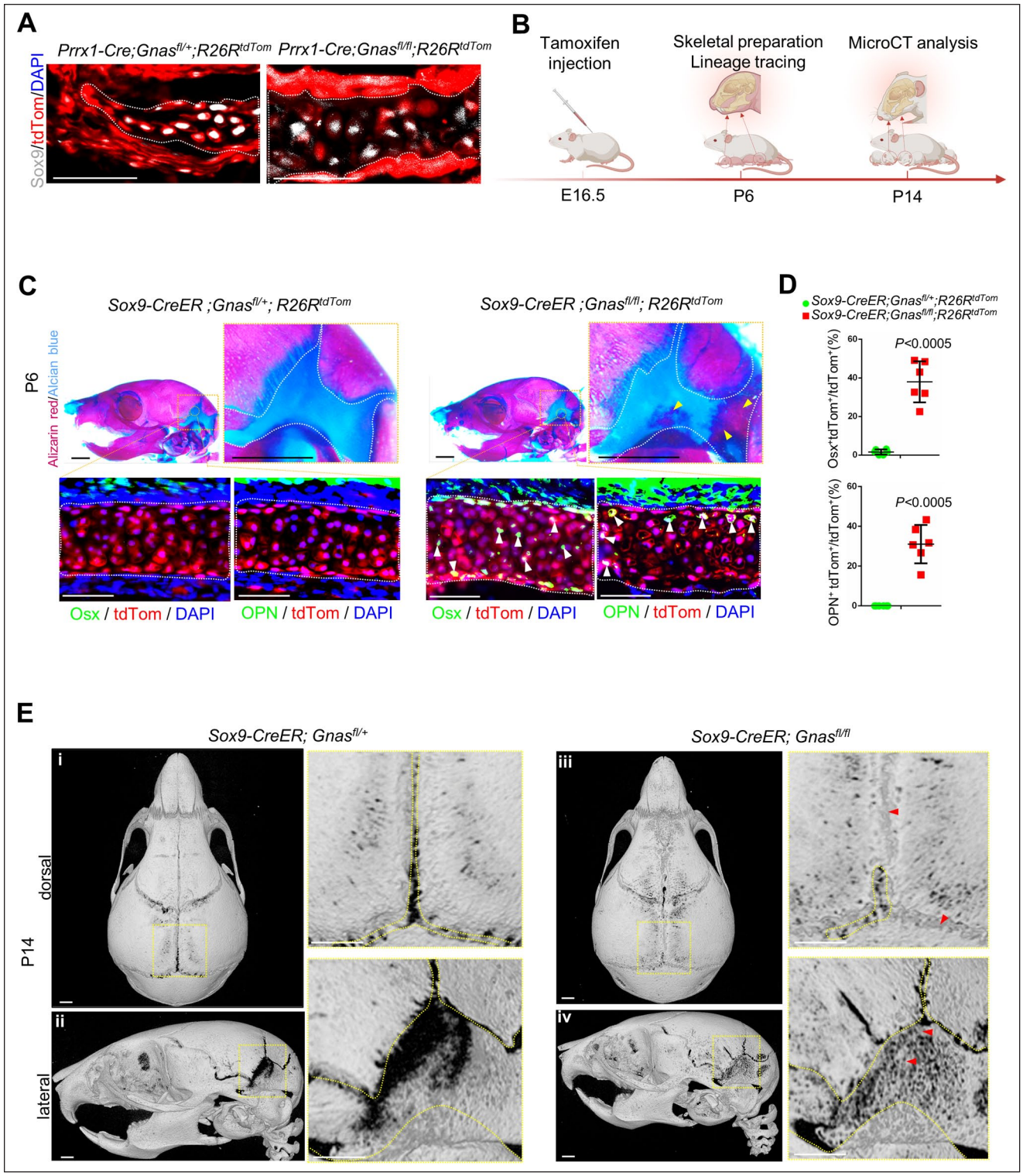

Figure 3. Sox9$^+$ chondrocyte-specific loss of *Gnas* replayed cranial cartilage heterotopic ossification (HO) and chondrocyte conversion. (**A**) Immunofluorescence staining of *Prrx1-Cre; Gnas$^{fl/fl}$; R26R^{Tomato}* and controls using Sox9 antibody at P0. (**B**) Schematics of experiment design. (**C**) Skeletal preparation of mouse calvarias from *Sox9-CreER; Gnas$^{fl/fl}$; R26R^{Tomato}* and their littermate controls (*Sox9-CreER; Gnas$^{fl/+}$; R26R^{Tomato}*) at P6. Mastoid fontanel is outlined in white. The yellow arrow indicates HO cartilage. Scale bar: 1 mm. Immunostaining using antibody of Osterix (Osx) and osteopontin (OPN) on serial sections. Outlined mutant cranial cartilage (tdTom) in an osteogenic differentiated status (Osx or OPN, green) indicated by arrows. Scale bar: 50 μm. (**D**) Quantification of suture cartilage in *Sox9-CreER; Gnas$^{fl/fl}$; R26R^{Tomato}*. Percentage of Osx$^+$tdTom$^+$ double positive cells and percentage of OPN$^+$tdTom$^+$ double positive cells, respectively, among total tdTom$^+$ chondrocytes at P6. $N = 6$, fields from 4 mice. Mean ± SD. Two-tailed *t* test. (**E**) Micro–computed tomography 3-dimensional reconstruction of *Sox9-CreER; Gnas$^{fl/fl}$* and their control littermates at P14. Dotted lines (yellow) outline patent sutures and fontanels; the arrow (red) indicates HO. Scale bar: 1 mm.

Loss of Gnas *Transformed Chondrocytes by Activating Hh Signaling*

To investigate whether the $G\alpha_s$-regulated cell fate alteration of cranial chondrocytes occurs through Hh signaling, we first crossed mice with the *Ptch1*^{LacZ} allele with *Prrx1-Cre; Gnas*$^{fl/fl}$ mice (Fig. 4A). Using whole-mount X-gal staining, we found that mutant sutures and fontanels showed extensive Hh activation compared to X-gal–negative controls (Fig. 4B, indicated by red arrow). Coronal sections of the mastoid fontanels of *Prrx1-Cre; Gnas*$^{fl/fl}$; *Ptch1*^{LacZ} mice showed a striking number of LacZ$^+$ chondrocytes, while the control cartilage contained no LacZ$^+$ cells (Fig. 4C, D). Through double staining with Safranin O and von Kossa, it was confirmed that unmineralized cartilage contained extensive LacZ$^+$ chondrocytes, which contributed to cartilage mineralization in *Prrx1-Cre; Gnas*$^{fl/fl}$; *Ptch1*^{LacZ} mice, while no LacZ$^+$ expression was observed in the control (Fig. 4E). These data indicate that $G\alpha_s$-regulated chondrocyte fate alteration is associated with the activation of Hh signaling within cranial cartilage.

Reduced Gli Transcription Activity Largely Rescued Cartilage Heterotopic Ossification

To determine whether Gli-dependent Hh signaling is required for ectopic ossification due to loss of *Gnas*, mice with the floxed *Gli2* allele (Bai et al. 2002)—the major Gli transcription factor that activates downstream targets of the Hh signaling pathway—were crossed with *Prrx1-Cre; Gnas*$^{fl/fl}$ mice to genetically downregulate Hh signaling. Micro-CT analyses revealed that the reduction of *Gli2* resulted in moderate changes in the mastoid fontanels of *Prrx1-Cre; Gli2*$^{fl/+}$ pups compared with controls at P0 (Fig. 5A). Cartilage mineralization within the mastoid fontanel was largely reduced in the calvaria of *Prrx1-Cre; Gnas*$^{fl/fl}$; *Gli2*$^{fl/+}$ mice, which was also confirmed by examining skeletal preparations (Fig. 5A). Immunostaining revealed that the chondrocytes of *Prrx1-Cre; Gnas*$^{fl/fl}$; *Gli2*$^{fl/+}$ mice presented a decreased expression of Osx by ~62% (Appendix Fig. 5A, B).

We administered Gli inhibitors to pregnant females and harvested the *Prrx1-Cre; Gnas*$^{fl/fl}$ pups and their littermates at P0 (Fig. 5B). GANT61 (see Appendix)—an antagonist inhibiting *Gli1*- and *Gli2*-induced transcription, downstream of Hh signaling—largely rescued cartilage mineralization in the mastoid fontanels of *Prrx1-Cre; Gnas*$^{fl/fl}$ mice compared with those of mutants that received dimethyl sulfoxide (DMSO) vehicle (Fig. 5C). Arsenic trioxide (ATO) (see Appendix)—another Gli inhibitor—also decreased cartilage ossification in the mastoid fontanels of *Prrx1-Cre; Gnas*$^{fl/fl}$ mice compared with those receiving vehicle (Fig. 5C). Therefore, loss of *Gnas* mostly resulted in *Gli*-dependent Hh signaling activation.

Overall, our data show that loss of *Gnas* results in cell-autonomous fate changes of chondrocytes into osteoblasts by activating Hh signaling, leading to cranial cartilage HO during premature suture fusion. Reduction of downstream Hh signal alleviates cranial cartilage HO. The $G\alpha_s$-Hedgehog signaling axis controls the identity of cranial chondrocytes in intramembranous ossification during calvaria development, providing insights for the development of Hh signaling therapy for craniosynostosis due to loss of *Gnas* (Fig. 5D).

Discussion

In bone research, the calvaria is frequently regarded as part of the skeleton with no distinction from long bones. In this study, we analyzed scRNA-seq data sets to reveal a unique Hh signaling activation pattern of cranial suture and used a genetic mouse model to demonstrate that $G\alpha_s$ protects this distinction by suppressing Hh signaling. Classically, normal intramembranous ossification in calvaria development concerns mesenchymal progenitor osteogenesis in the absence of cranial cartilage. Unexpectedly, loss of *Gnas* causes the cranial cartilage to lose its distinctiveness and be evoked to ossify through hypertrophy during pathological intramembranous ossification, expanding the theory of craniosynostosis. Our study clarifies the crucial role of $G\alpha_s$ in controlling osteogenic potential of cranial chondrocytes in the orchestration of intramembranous ossification during calvaria development (Fig. 5D).

POH is thought to arise directly from mesenchymal cells that stimulate HO through pathological intramembranous ossification in the absence of ectopic cartilage, as we have previously reported (Xu, Hu, et al. 2018; Xu, Khan, et al. 2018; Cong et al. 2019). Comparatively, fibrodysplasia ossificans progressiva (FOP, OMIM #135100) due to mutations in *ACVR1*, occurs through heterotopic endochondral ossification and is closely related to bone morphogenetic proteins (BMPs) signaling, which originates from the endothelial-to-mesenchymal transition (Medici et al. 2010; Shoshani and Zipori 2011; Kaplan et al. 2020). Notably, loss of *Gnas* triggers heterotopic osteochondrogenic disorders within cranial cartilage during calvaria development, supporting the uniqueness of POH from FOP. This disordered osteochondrogenesis is robust in mutant *Prrx1-Cre; R26R*^{Tomato}; *Gnas*$^{fl/fl}$ chondrocytes, extensively triggered in mutant *Sox9-CreER; R26R*^{Tomato}; *Gnas*$^{fl/fl}$ chondrocytes, and nonexistent in normal chondrocytes with mutant *Osx-Cre; Gnas*$^{fl/fl}$ osteoblasts (Figs. 2 and 3, Appendix Fig. 1). Together with accelerated osteogenic expansion and ectopic ossification in suture mesenchyme (Xu, Khan, et al. 2018), our findings underpin the cellular mechanism by which the chondrocyte-to-osteoblast transition gives rise to cranial cartilage HO, providing hints for the underlying mechanisms of craniosynostosis skull deformity in POH. This animal model recapitulates skull deformity but is still not completely equivalent to craniosynostosis by loss of *GNAS* in POH patients. Future mechanism exploration is greatly needed.

Craniosynostosis due to gene mutation is hard to completely rectify. We mainly focused on the embryonic/neonatal stage of craniosynostosis in the mouse model and tried to explore early interventions as a preventive method to avoid cranial suture HO formation. Recent literature has reported the essential role of adult mouse suture mesenchymal stem/progenitors in the regeneration of functional sutures after craniosynostosis in a mouse model. Cranial suture Gli1$^+$ mesenchymal stem cells (MSCs) support coronal suture regeneration

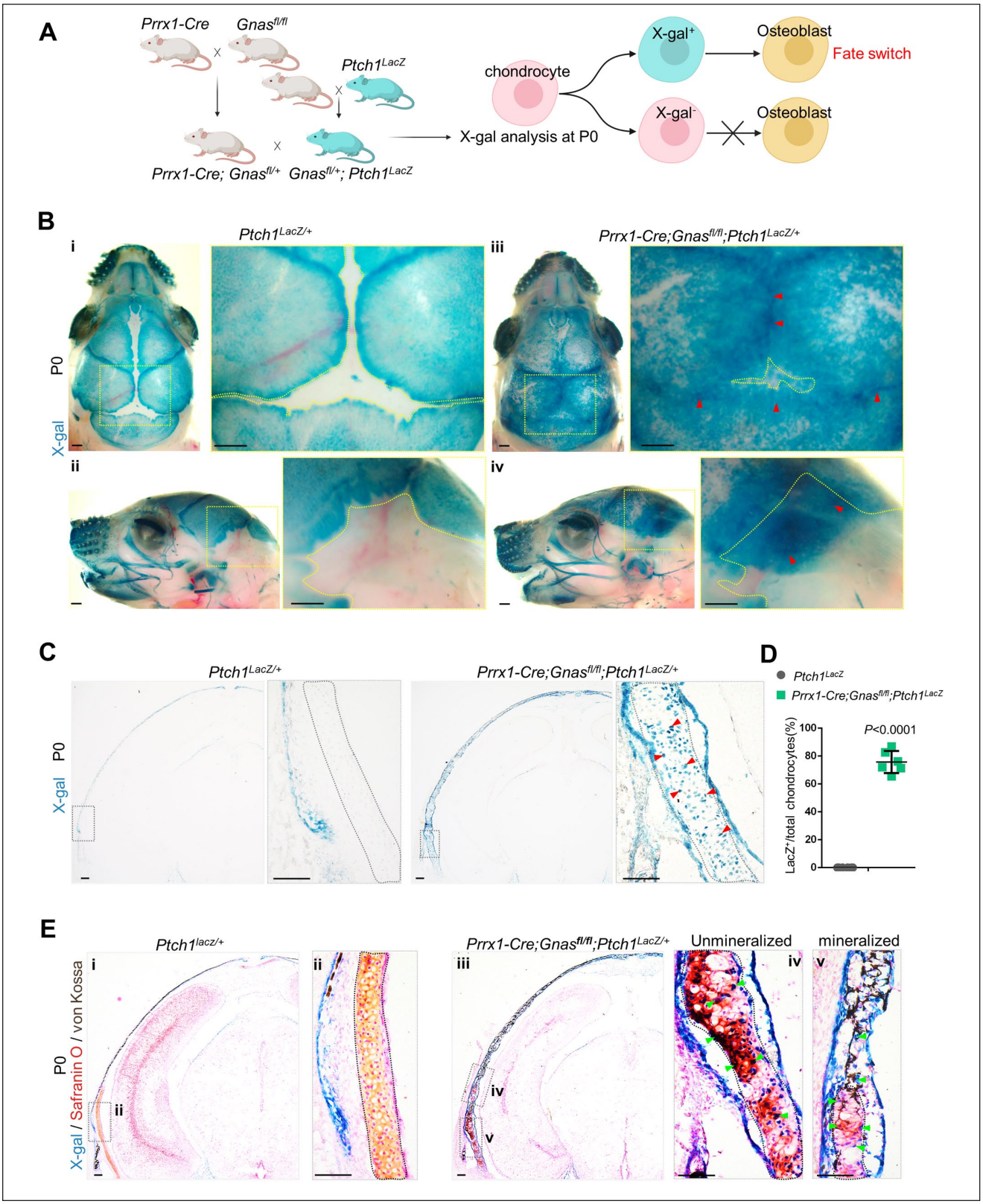

Figure 4. Loss of *Gnas* transformed chondrocytes by activating Hedgehog (Hh). (**A**) Schematics of mice mating. (**B**) Whole-mount X-gal staining of *Prrx1-Cre; Gnas*$^{fl/fl}$; *Ptch1*^{LacZ} mouse and control littermate calvarias. The arrow (red) indicates ectopic X-gal (green) in outlined sutures and fontanels. Scale bar: 0.5 mm. (**C**) X-gal staining on coronal cryostat sections of *Prrx1-Cre; Gnas*$^{fl/fl}$; *Ptch1*^{LacZ} mouse calvaria. The arrow (red) indicates X-gal^{+} chondrocytes (green) in the outlined cartilage. Scale bar: 100 μm. (**D**) Quantification of X-gal staining. Percentage of X-gal^{+} chondrocytes among total chondrocytes. $N = 6$ mice. Mean ± SD. Two-tailed t test. (**E**) Costaining with Safranin O and von Kossa on X-gal staining of *Prrx1-Cre; Gnas*$^{fl/fl}$; *Ptch1*^{LacZ} mouse and control littermate calvarias. The arrow (green) indicates X-gal^{+} chondrocytes contributing to the mineralization of mutant cartilage (outlined). Scale bar: 100 μm.

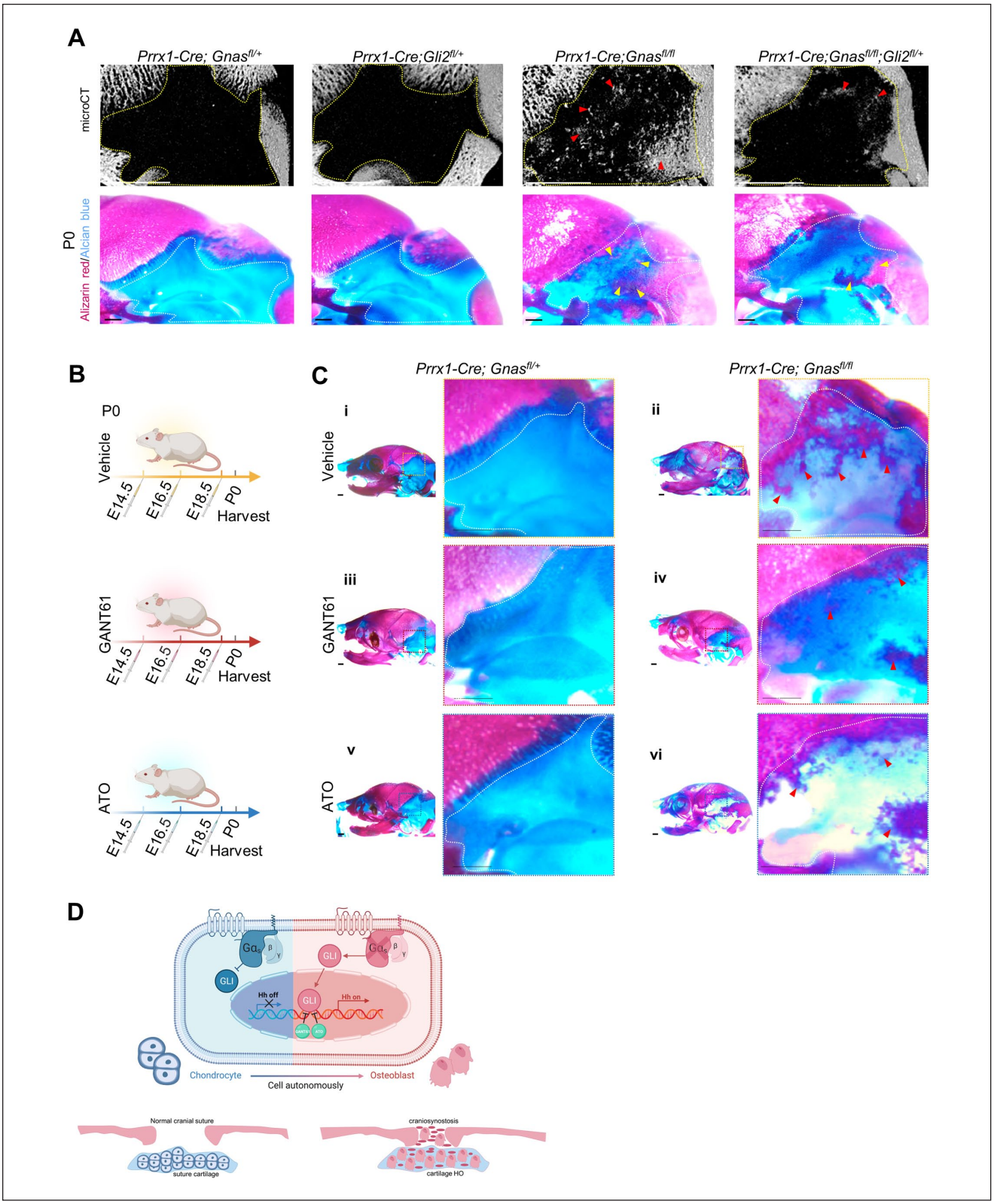

Figure 5. Reduction of Gli transcription activity largely rescued cartilage ossification. (**A**) Upper: micro–computed tomography 3-dimensional image of *Prrx1-Cre; Gnas*$^{fl/fl}$; *Gli2*$^{fl/+}$ mouse and the control littermate calvarias. Dotted lines outline enlarged view of mastoid fontanel. The arrows (red) indicate reduced heterotopic ossification (HO). Scale bars: 1 mm. Lower: skeletal preparation of mouse calvarias and their control littermates. The arrows (yellow) indicate reduced HO in rescue group. Scale bar: 1 mm. (**B**) Schematics of experiment design. (**C**) Skeletal preparation of mouse calvarias receiving GANT61, ATO, or DMSO (vehicle). The arrows (red) indicate reduced HO. Scale bar: 1 mm. (**D**) Schematics of this work: a $G\alpha_s$-regulated conversion of cranial chondrocyte identity through Hedgehog signaling strengthens HO during calvaria development.

and effectively prevent resynostosis 6 mo after transplantation using the craniosynostosis model *Twist1*$^{+/-}$ mice (Yu et al. 2021). Enhanced Wnt activation by crossing with *Axin2*$^{LacZ/+}$ enriches suture mesenchymal stem/progenitor cells and restores cranial suture patency in P15 and 6-mo-old craniosynostosis model *Twist1*$^{+/-}$ mice (Menon et al. 2021). Delayed bone formation of calvaria bone elements was shown at P0, and evident HO within the suture mesenchyme was observed at P7 in *Axin2*$^{Cre\text{-}Dox}$; *Bmpr1a*$^{fl/fl}$ mice induced from E16.5 (Maruyama et al. 2021). Bmpr1a plays a role in suture mesenchymal cell self-renewal and osteogenesis during normal suture formation (Maruyama et al. 2021). From our data, we can infer that early correction of Hh signaling activation as a preventive method partially inhibits progressive HO within the cranial suture in loss-of-*Gnas* mice by hindering neonatal cranial chondrocyte transformation.

Author Contributions

R. Xu, contributed to conception, design, data acquisition, analysis, and interpretation, drafted and critically revised the manuscript; Y. Liu, Y. Zhou, contributed to design, data acquisition, and analysis, drafted the manuscript; W. Lin, contributed to design, data analysis, and interpretation, drafted the manuscript; Q. Yuan, contributed to conception, design, data analysis and interpretation, critically revised the manuscript; X. Zhou, contributed to conception, design, and data interpretation, critically revised the manuscript; Y. Yang, contributed to conception, design, data acquisition, and interpretation, critically revised the manuscript. All authors gave their final approval and agreed to be accountable for all aspects of the work.

Acknowledgments

We thank the Yang lab members for discussions and collaboration, MicroCT Core of Harvard School of Dental Medicine for technical support, and the Bone Biology platform and Oral Health platform of State Key Laboratory of Oral Diseases. We thank Dorothy Hu from Harvard School of Dental Medicine for instructions of preparation of undecalcified hard tissues. Schematics were created with BioRender.com.

Declaration of Conflicting Interests

The authors declared no potential conflicts of interest with respect to the research, authorship, and/or publication of this article.

Funding

The authors disclosed receipt of the following financial support for the research, authorship, and/or publication of this article: This work was supported by National Institutes of Health grants from the National Institute of Dental and Craniofacial Research (R01DE025866) and from National Institute of Arthritis and Musculoskeletal and Skin Diseases (R01AR070877) to Y. Yang and National Natural Science Foundation of China (82001001), China Postdoctoral Science Foundation (BX20190224), Innovation Program of Chengdu City (2019-YF05-01236-SN), Postdoctoral Foundation of Sichuan University (2020SCU12018), and Research Funding of West China Hospital of Stomatology (RCDWJS2020- 21, RD-02-202101) to R. Xu.

Data Availability

The scRNA-seq data sets of cranial sutures can be download from fasebase (https://www.facebase.org/x, doi:10.1016/j.celrep.2020.107871) with accession number FB00001013 (Holmes et al. 2020). The scRNA-seq data for limbs can be download from Gene Expression Omnibus (https://www.ncbi.nlm.nih.gov/geo/, doi:10.1016/j.matbio.2019.12.004) with GEO accession number GSE 142425 (Kelly et al. 2020).

References

Bai CB, Auerbach W, Lee JS, Stephen D, Joyner AL. 2002. Gli2, but not Gli1, is required for initial Shh signaling and ectopic activation of the Shh pathway. Development. 129(20):4753–4761.

Chen M, Gavrilova O, Zhao WQ, Nguyen A, Lorenzo J, Shen L, Nackers L, Pack S, Jou W, Weinstein LS. 2005. Increased glucose tolerance and reduced adiposity in the absence of fasting hypoglycemia in mice with liver-specific Gs α deficiency. J Clin Invest. 115(11):3217–3227.

Cong Q, Liu Y, Zhou T, Zhou Y, Xu R, Cheng C, Chung HS, Yan M, Zhou H, Liao Z, et al. 2021. A self-amplifying loop of YAP and SHH drives formation and expansion of heterotopic ossification. Sci Transl Med. 13(599):eabb2233.

Cong Q, Xu R, Yang Y. 2019. $G\alpha_s$ signaling in skeletal development, homeostasis and diseases. Curr Top Dev Biol. 133:281–307.

Corrales JD, Blaess S, Mahoney EM, Joyner AL. 2006. The level of sonic hedgehog signaling regulates the complexity of cerebellar foliation. Development. 133(9):1811–1821.

Fresard L, Smail C, Ferraro NM, Teran NA, Li X, Smith KS, Bonner D, Kernohan KD, Marwaha S, Zappala Z, et al. 2019. Identification of rare-disease genes using blood transcriptome sequencing and large control cohorts. Nat Med. 25(6):911–919.

Frost ER, Taylor G, Baker MA, Lovell-Badge R, Sutherland JM. 2021. Establishing and maintaining fertility: the importance of cell cycle arrest. Genes Dev. 35(9–10):619–634.

Gong X, Qian H, Cao P, Zhao X, Zhou Q, Lei J, Yan N. 2018. Structural basis for the recognition of sonic hedgehog by human patched1. Science. 361(6402):eaas8935.

Graul-Neumann LM, Bach A, Albani M, Ringe H, Weimann A, Kress W, Hiort O, Bartsch O. 2009. Boy with pseudohypoparathyroidism type 1a caused by GNAS gene mutation (deltaN377), Crouzon-like craniosynostosis, and severe trauma-induced bleeding. Am J Med Genet A. 149A(7):1487–1493.

Hagelstein-Rotman M, Meier ME, Majoor BCJ, Cleven AHG, Dijkstra PDS, Hamdy NAT, van de Sande MAJ, Dekkers OM, Appelman-Dijkstra NM. 2021. Increased prevalence of malignancies in fibrous dysplasia/McCune-Albright syndrome (FD/MAS): data from a National Referral Center and the Dutch National Pathology Registry (PALGA). Calcif Tissue Int. 108(3):346–353.

Holmbeck K, Bianco P, Chrysovergis K, Yamada S, Birkedal-Hansen H. 2003. MT1-MMP-dependent, apoptotic remodeling of unmineralized cartilage: a critical process in skeletal growth. J Cell Biol. 163(3):661–671.

Holmes G, Gonzalez-Reiche AS, Lu N, Zhou X, Rivera J, Kriti D, Sebra R, Williams AA, Donovan MJ, Potter SS, et al. 2020. Integrated transcriptome and network analysis reveals spatiotemporal dynamics of calvarial suturogenesis. Cell Rep. 32(1):107871.

Hu Q, Shokat KM. 2018. Disease-causing mutations in the G protein Gαs subvert the roles of GDP and GTP. Cell. 173(5):1254–1264 e1211.

Kaplan FS, Al Mukaddam M, Stanley A, Towler OW, Shore EM. 2020. Fibrodysplasia ossificans progressiva (FOP): a disorder of osteochondrogenesis. Bone. 140:115539.

Kelly NH, Huynh NPT, Guilak F. 2020. Single cell RNA-sequencing reveals cellular heterogeneity and trajectories of lineage specification during murine embryonic limb development. Matrix Biol. 89:1–10.

Khan SK, Yadav PS, Elliott G, Hu DZ, Xu R, Yang Y. 2018. Induced Gnas(R201H) expression from the endogenous Gnas locus causes fibrous dysplasia by up-regulating Wnt/β-catenin signaling. Proc Natl Acad Sci U S A. 115(3):E418–E427.

Leclercq V, Benoit V, Lederer D, Delaunoy M, Ruiz M, de Halleux C, Robaux O, Wanty C, Maystadt I. 2018. Case report: an infantile lethal form of

Albright hereditary osteodystrophy due to a GNAS mutation. Clin Case Rep. 6(10):1933–1940.
Logan M, Martin JF, Nagy A, Lobe C, Olson EN, Tabin CJ. 2002. Expression of Cre recombinase in the developing mouse limb bud driven by a Prxl enhancer. Genesis. 33(2):77–80.
Mak KK, Chen MH, Day TF, Chuang PT, Yang Y. 2006. Wnt/beta-catenin signaling interacts differentially with Ihh signaling in controlling endochondral bone and synovial joint formation. Development. 133(18):3695–3707.
Martik ML, Gandhi S, Uy BR, Gillis JA, Green SA, Simoes-Costa M, Bronner ME. 2019. Evolution of the new head by gradual acquisition of neural crest regulatory circuits. Nature. 574(7780):675–678.
Maruyama T, Stevens R, Boka A, DiRienzo L, Chang C, Yu HI, Nishimori K, Morrison C, Hsu W. 2021. BMPR1A maintains skeletal stem cell properties in craniofacial development and craniosynostosis. Sci Transl Med. 13(583):eabb4416.
Massimi L, Bianchi F, Frassanito P, Calandrelli R, Tamburrini G, Caldarelli M. 2019. Imaging in craniosynostosis: when and what? Childs Nerv Syst. 35(11):2055–2069.
Medici D, Shore EM, Lounev VY, Kaplan FS, Kalluri R, Olsen BR. 2010. Conversion of vascular endothelial cells into multipotent stem-like cells. Nat Med. 16(12):1400–1406.
Menon S, Salhotra A, Shailendra S, Tevlin R, Ransom RC, Januszyk M, Chan CKF, Behr B, Wan DC, Longaker MT, et al. 2021. Skeletal stem and progenitor cells maintain cranial suture patency and prevent craniosynostosis. Nat Commun. 12(1):4640.
Minoux M, Holwerda S, Vitobello A, Kitazawa T, Kohler H, Stadler MB, Rijli FM. 2017. Gene bivalency at polycomb domains regulates cranial neural crest positional identity. Science. 355(6332):eaal2913.
Newton PT, Li L, Zhou B, Schweingruber C, Hovorakova M, Xie M, Sun X, Sandhow L, Artemov AV, Ivashkin E, et al. 2019. A radical switch in clonality reveals a stem cell niche in the epiphyseal growth plate. Nature. 567(7747):234–238.
Ono N, Ono W, Nagasawa T, Kronenberg HM. 2014. A subset of chondrogenic cells provides early mesenchymal progenitors in growing bones. Nat Cell Biol. 16(12):1157–1167.
Rodda SJ, McMahon AP. 2006. Distinct roles for Hedgehog and canonical Wnt signaling in specification, differentiation and maintenance of osteoblast progenitors. Development. 133(16):3231–3244.
Shore EM, Ahn J, Jan de Beur S, Li M, Xu M, Gardner RJ, Zasloff MA, Whyte MP, Levine MA, Kaplan FS. 2002. Paternally inherited inactivating mutations of the GNAS1 gene in progressive osseous heteroplasia. N Engl J Med. 346(2):99–106.
Shoshani O, Zipori D. 2011. Transition of endothelium to cartilage and bone. Cell Stem Cell. 8(1):10–11.
Soeda T, Deng JM, de Crombrugghe B, Behringer RR, Nakamura T, Akiyama H. 2010. Sox9-expressing precursors are the cellular origin of the cruciate ligament of the knee joint and the limb tendons. Genesis. 48(11):635–644.
Tambuyzer E, Vandendriessche B, Austin CP, Brooks PJ, Larsson K, Miller Needleman KI, Valentine J, Davies K, Groft SC, Preti R, et al. 2020. Therapies for rare diseases: therapeutic modalities, progress and challenges ahead. Nat Rev Drug Discov. 19(2):93–111.
Vercauteren Drubbel A, Pirard S, Kin S, Dassy B, Lefort A, Libert F, Nomura S, Beck B. 2021. Reactivation of the Hedgehog pathway in esophageal progenitors turns on an embryonic-like program to initiate columnar metaplasia. Cell Stem Cell. 28(8):1411–1427.e7.
Wang L, Mishina Y, Liu F. 2015. Osterix-Cre transgene causes craniofacial bone development defect. Calcif Tissue Int. 96(2):129–137.
Warren SM, Brunet LJ, Harland RM, Economides AN, Longaker MT. 2003. The BMP antagonist noggin regulates cranial suture fusion. Nature. 422(6932):625–629.
Xu R, Hu J, Zhou X, Yang Y. 2018. Heterotopic ossification: mechanistic insights and clinical challenges. Bone. 109:134–142.
Xu R, Khan SK, Zhou T, Gao B, Zhou Y, Zhou X, Yang Y. 2018. Gαs signaling controls intramembranous ossification during cranial bone development by regulating both hedgehog and Wnt/β-catenin signaling. Bone Res. 6:33.
Yu M, Ma L, Yuan Y, Ye X, Montagne A, He J, Ho TV, Wu Y, Zhao Z, Sta Maria N, et al. 2021. Cranial suture regeneration mitigates skull and neurocognitive defects in craniosynostosis. Cell. 184(1):243–256.e18.